ACTA PHYSIOLOGICA

Acta Physiol 2014, **211**, 36–47

Ventricular remodelling in rabbits with sustained high-fat diet

M. Zarzoso,[1,2] S. Mironov,[1] G. Guerrero-Serna,[1] B. Cicero Willis[1] and S. V. Pandit[1]

1 Center for Arrhythmia Research, University of Michigan, Ann Arbor, MI, USA

2 Department of Physiotherapy, Universitat de València, Valencia, Spain

Received 2 July 2013,
revision requested 2 September 2013,
revision received 8 October 2013,
accepted 19 October 2013
Correspondence: S. V. Pandit, Center for Arrhythmia Research, University of Michigan, NCRC, Bldg. 26-2L01N, 2800, Plymouth Road, Ann Arbor, MI 48109, USA.
E-mail: sanpandi@med.umich.edu

Abstract

Aim: Excess weight gain and obesity are one of the most serious health problems in the western societies. These conditions enhance risk of cardiac disease and have been linked with increased prevalence for cardiac arrhythmias and sudden death. Our goal was to study the ventricular remodelling occurring in rabbits fed with high-fat diet (HFD) and its potential arrhythmogenic mechanisms.

Methods: We used 15 NZW rabbits that were randomly assigned to a control ($n = 7$) or HFD group ($n = 8$) for 18 weeks. *In vivo* studies included blood glucose, electrocardiographic, and echocardiographic measurements. Optical mapping was performed in Langendorff-perfused isolated hearts.

Results: Body weight (3.69 ± 0.31 vs. 2.94 ± 0.18 kg, $P < 0.001$) and blood glucose levels (230 ± 61 vs. 141 ± 14 mg dL^{-1}, $P < 0.05$) were higher in the HFD group vs. controls. The rate-corrected QT interval and its dispersion were increased in HFD rabbits vs. controls (169 ± 10 vs. 146 ± 13 ms and 37 ± 11 vs. 9 ± 2 ms, respectively; $P < 0.05$). Echocardiographic analysis showed morphological and functional alterations in HFD rabbits indicative of left ventricle (LV) hypertrophy. Isolated heart studies revealed no changes in repolarization and propagation properties under conditions of normal extracellular K^+, suggesting that extrinsic factors could underlie those electrocardiographic modifications. There were no differences in the dynamics of ventricular fibrillation (frequency, wave breaks) in the presence of isoproterenol. However, HFD rabbits showed a small reduction in action potential duration and an increased incidence of arrhythmias during hyperkalaemia.

Conclusion: High-fat feeding during 18 weeks in rabbits induced a type II diabetes phenotype, LV hypertrophy, abnormalities in repolarization and susceptibility to arrhythmias during hyperkalaemia.

Keywords high-fat diet, ventricle structure and electrophysiology.

The epidemic of obesity and excess weight gain is increasing worldwide and has been linked to an enhanced risk of cardiovascular disease and mortality (Van Gaal *et al.* 2006, Lavie *et al.* 2009, Nduhirabandi *et al.* 2012). Obesity is associated with a variety of abnormalities in the ECG including a prolonged QT interval (Fraley *et al.* 2005), increased QT dispersion (Fraley *et al.* 2005) and a greater incidence of premature ventricular complexes (Messerli *et al.* 1987). High-fat diet that results in the development of insulin resistance and obesity has been also linked with structural and functional remodelling, leading to cardiac hypertrophy and left ventricular (LV) dysfunction (Messerli *et al.* 1987, Lavie *et al.* 2009). Collectively,

 doi: 10.1111/apha.12185

these structural and electrical changes could constitute a potential substrate for the development of lethal ventricular arrhythmias. Indeed, an increased risk of arrhythmias and sudden death with increasing body weight has been reported (Messerli *et al.* 1987, Kannel *et al.* 1988, Lakhani & Fein 2011), but the underlying mechanisms remain poorly understood.

Animal models of excess weight and obesity, particularly rodent (rat, mouse) models, have provided valuable insights regarding the mechanisms involved in the pathophysiological abnormalities of the heart during the onset of obesity (Lin *et al.* 2012, Persson & Persson 2012, Huang *et al.* 2013). However, in the context of studying the electrophysiological remodelling, small rodent models have many limitations. The murine ventricle displays a short triangular action potential (approx. 50 ms) and lacks the key repolarizing ion channels that are present in the human ventricle, that is, the fast and the slow delayed rectifier K^+ currents (I_{Kr} and I_{Ks}) (Nerbonne & Kass 2005, Killeen *et al.* 2008). In contrast, in the rabbit ventricular myocardium, the action potential morphology is spike and dome shaped, the duration is approx. 200–300 ms, and the repolarization is mainly mediated by I_{Kr} and I_{Ks}, which is similar to that seen in the human ventricle (Lengyel *et al.* 2001, 2008, Torres-Jacome *et al.* 2013). Further, the rabbit model has been widely used for studying sustained arrhythmias and ventricular fibrillation (VF) (Such *et al.* 2008, Noujaim *et al.* 2010, Zarzoso *et al.* 2012). It has also been shown in previous studies that rabbits placed on a high-fat diet exhibit many of the characteristics of obesity seen in humans (Carroll *et al.* 1996), and lipid metabolism in obese rabbits is also similar to that of obese humans (Zhang *et al.* 2008). Therefore, our main goal was to study the functional and electrophysiological alterations occurring in the ventricular myocardium in a rabbit model of obesity.

Methods and procedures

The study complied with Good Publishing Practice in Physiology (Persson & Henriksson 2011). The methods are outlined in the following sections (see Supporting Information for details).

Animals and diet

Experiments were performed using 15 New Zealand White, male rabbits (10–11 weeks old, 2.33 ± 0.12 Kg at the beginning of the study). Animal-handling protocols conformed to United States National Institutes of Health Guidelines and the European (D2003/65/CE and R2007/526/CE) Guidelines for the Care of Animals Used in Experimental and other Research Purposes and were approved by the University Committee on Use and Care of Animals of the University of Michigan.

After a period of 2 weeks of acclimatization, the rabbits were randomly assigned to the control group ($n = 7$), fed with the normal chow, or to the experimental group (HFD; $n = 8$), fed with a high-fat diet which consisted of the standard rabbit chow with an additional 15% fat (10% corn oil and 5% lard, Research Diets, see Supporting Information for details), as described in a previous study by Carroll *et al.* (1996). Both groups were kept on their respective diets for approx. 18 weeks.

Morphological measurements

Weight, length, body mass index (BMI), abdominal circumference and abdominal circumference/body length ratio were determined.

Intravenous glucose tolerance test (IVGTT)

For the evaluation of glucose metabolism, IVGTT was performed as previously described by Koike *et al.* (2004). Blood glucose was measured with a glucose meter (Precision Xtra, Abbot Diabetes Care). The area under the curve (AUC) was calculated by multiplying the cumulative mean height of glucose (mg dL^{-1}) by the time (hours) (Liu *et al.* 2005).

Echocardiographic study

Transthoracic echocardiography was performed as in earlier studies (Herron *et al.* 2010), before and 18 weeks after starting the high-fat diet, using Vevo 2100 ultrasound system (Visualsonics, Toronto, ON, Canada) with a MS200 9–18 MHz Cardiovascular MicroScan transducer. The description of the parameters studied can be found in the Supporting Information (Supplemental Table S2).

Electrocardiographic study

ECG recordings (500 s) were made by means of two standard bipolar leads connected to a P511 amplifier (Grass Technologies) with a sampling rate of 1 kHz. P-P and R-R intervals, P-wave duration and dispersion, QRS duration, P-R interval and corrected QT interval and dispersion were analysed with Clampfit ver.10.2.0.12 (Molecular Devices, Sunnyvale, CA, USA). The mean value of 25 consecutive beats was used in each animal for quantification. Additionally, we quantified short-term heart rate variability (HRV) in 500 s recordings. Time domain, geometrical and nonlinear standard HRV parameters were quantified

using Kubios HRV software (Niskanen *et al.* 2004): standard deviation of the R-R (RRSD), square root of the mean squared differences of successive R-R intervals (RMSSD), percentage of the successive R-R intervals that differ by more than 50 ms (pNN50), R-R triangular index (HRVI), the triangular interpolation of the R-R interval histogram (TIRR), and the SD1-SD2 descriptors of the Poincaré plot. A more detailed description of the parameters studied can be found in the Supporting Information (Supplemental Table S3).

*Electrophysiological studies (*in vitro*)*

Optical mapping was performed as described in previous studies (Pandit *et al.* 2011a,b). Briefly, after the administration of anaesthesia, hearts were quickly removed and immersed in cold (4 °C) cardioplegic solution for further preparation. The aorta was cannulated and connected to a Langendorff system to provide the heart with warmed, oxygenated Tyrode's solution. Oxygenation was carried out with a mixture of 95% O_2 and 5% CO_2. The heart was immersed in the same Tyrode's solution, in a custom-made plastic chamber, and the temperature was maintained at 35.5 ± 1.5 °C. The perfusion pressure was maintained between 60 and 70 mm Hg. Blebbistatin (5–10 μmol L^{-1}, Sigma, St. Louis, MO, USA) was added to the perfusate to minimize motion artefact (Fedorov *et al.* 2007, Brines *et al.* 2012). A 1–2 mL bolus of the voltage-sensitive dye Di-4-ANEPPS (10 μmol L^{-1}, Sigma) was added to the perfusion line. Optical movies were recorded using a high-resolution 80 × 80 pixel Little Joe CCD camera at 1 kHz sampling frequency.

Stimulation was performed by means of a bipolar electrode positioned on the right ventricle epicardium near the outflow tract. Electrical stimuli with intensity two times the diastolic threshold were delivered by an A310 Accupulser stimulator (World Precision Instruments, Sarasota, FL, USA) connected to a stimulus isolation unit (A385, World Precision Instruments). Volume-conducted ECGs (pseudo lead 1) were digitized at 1 KHz using a P511 AC amplifier (Grass Technologies, Warwick, RI, USA). The hearts were paced at 250, 225, 200, 175, 150, 125, and 100 ms cycle length in normo- and hyperkalaemia (4, and 12 mmol L^{-1} $[K^+]_o$ respectively), and during perfusion with the beta-adrenergic agonist isoproterenol (100 nmol L^{-1}). Ventricular fibrillation (VF) was induced by pacing at increasing frequencies (2 Hz s^{-1}) in the presence of isoproterenol. Optical action potential duration (APD) at 80% of repolarization (APD_{80}), conduction velocity (CV), dominant frequency (DF), regularity index (RI) and singularity points density (SPD) measurements were made as in previous studies (Kalifa *et al.* 2006, Pandit *et al.* 2010, Zarzoso *et al.* 2013).

Plasma measurements

Post-heparin plasma was collected from rabbits at week 18. Triglycerides (TG), total cholesterol (TC) and high-density lipoprotein (HDL) cholesterol were determined.

Statistical analysis

Values are reported as mean ± standard deviation, unless stated otherwise. A repeated measures analysis of variance model with Bonferroni test for multiple comparisons and unpaired t-test were used when appropriate (SPSS, NY, USA, version 17.0 for Windows). Differences were considered significant at a two-tailed alpha level of $P < 0.05$.

Results

Morphological parameters and lipid profile

There was a progressive weight gain in HFD group that started to diverge from the control group as early as the 4th week (Fig. 1a). By the end of the 18th week, the HFD group showed a 25.3% increase in body weight compared with controls (2.94 ± 0.18 vs. 3.69 ± 0.31 Kg, $P < 0.001$, Table 1). While there were no differences between the two groups in the body length at the end of the study, we found a significant increase in BMI (15.52 ± 1.72 vs. 19.37 ± 1.20 Kg m^{-2}, $P < 0.001$), abdominal circumference (314 ± 13 vs. 363 ± 19 mm, $P < 0.001$), and abdominal circumference/body length ratio (0.72 ± 0.07 vs. 0.83 ± 0.04, $P < 0.01$) in the HFD group (Table 1). Analyses of the plasma lipid profile showed that even though the mean values of TC, HDL and TG tended to be higher in the HFD-fed animals, they were not significantly different between both groups (Fig. 1b).

Effects of HFD feeding on glucose metabolism

The random plasma glucose measurements showed similar levels between the control and HFD group immediately before starting the diet (133 ± 14 vs. 144 ± 13 mg dL^{-1}). After 18 weeks of HFD feeding, while the values in the control group remained similar to the initial plasma glucose levels, we found a significant increase in the in the HFD group compared with controls (230 ± 61 vs. 141 ± 14 mg dL^{-1}, $P < 0.05$; Fig. 2a). Additionally, an IVGTT was performed after 18 weeks. After overnight fasting, resting plasma glucose levels were similar between the two groups

  doi: 10.1111/apha.12185

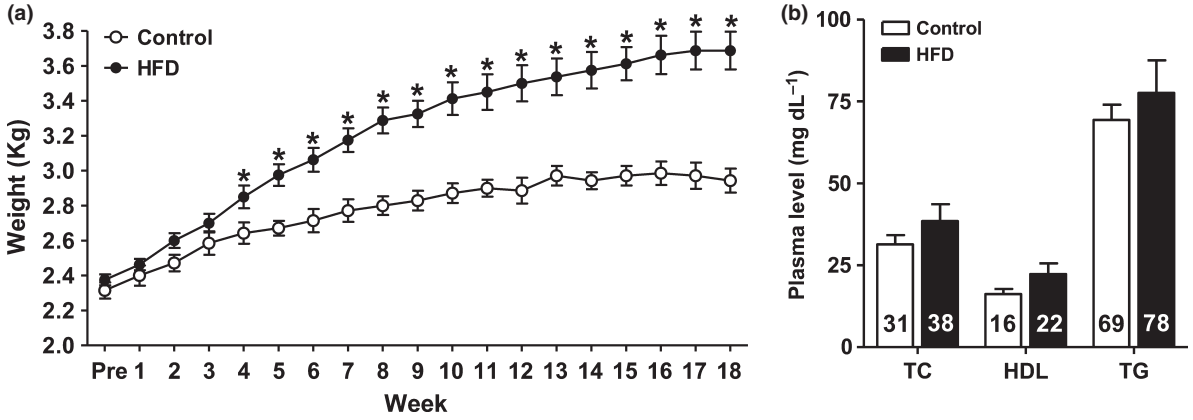

Figure 1 Weight and lipid profile. (a) Evolution of the weight in control (n = 7) and HFD (n = 8) groups from the start of the study to the 18th week in their respective diets. (b) Lipid profile showing total cholesterol (TC), high-density lipoprotein (HDL) and triglycerides (TG) at the end of the study Control group n = 6, HFD group n = 7. Error bars display the SEM. *P < 0.05 vs control.

Table 1 Morphological characteristics of the rabbits at the end of the study (18 weeks)

	Control	HFD
Body weight (Kg)	2.94 ± 0.18	3.69 ± 0.31**
Body length (mm)	437 ± 31	436 ± 14
BMI (Kg m^{-2})	15.52 ± 1.72	19.37 ± 1.20**
Abdominal circumference (mm)	314 ± 13	363 ± 19**
Abdominal circumference/body length	0.72 ± 0.07	0.83 ± 0.04*

BMI, body mass index. Data are presented as mean ± SD.
*P < 0.01.
**P < 0.001.

(153 ± 27 vs. 169 ± 17 mg dL^{-1}), but HFD-fed rabbits showed a higher value, and a slower rate of glucose clearance from the blood than control animals, at all the time points studied after 15 min of intravenous glucose injection (Fig. 2b). After 240 min, animals in the control group showed plasma glucose levels similar to basal (154 ± 24 mg dL^{-1}). However, this parameter remained increased in the HFD group (247 ± 62 mg dL^{-1}, P < 0.05 vs. control). The AUC calculated from the IVGTT was significantly increased in the HFD group (1599 ± 211 vs. 1.841 ± 189 mg dL^{-1} h, P < 0.05, Fig. 2c).

Changes in the ECG produced by the HFD

The electrocardiographic parameters are shown in Fig. 3. There were no differences in the heart rate between control and HFD groups, as shown by the P-P interval duration (Panel a), before (389 ± 34 vs. 409 ± 49 ms) and after the 18 weeks (403 ± 52 vs. 380 ± 56 ms). While we found no differences in QRS duration (48 ± 3 vs. 48 ± 6 ms) or P-R interval (69 ± 4 vs. 70 ± 8 ms) between control and HFD groups after 18 weeks, corrected QT interval (QTc)

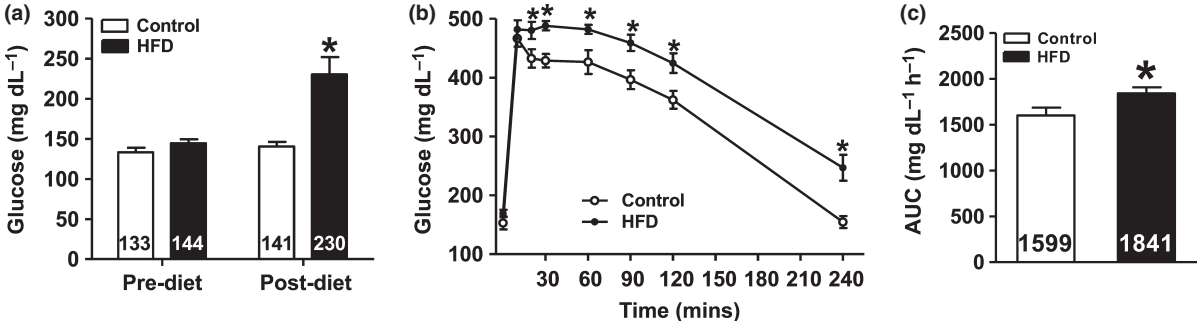

Figure 2 Effects of HFD feeding on glucose metabolism. (a) Plasma glucose level after random measurements. (b) Glucose levels during the intravenous glucose tolerance test after overnight fasting. (c) Area under the curve (AUC) calculated multiplying the cumulative mean height of glucose by the time. Control n = 7, HFD n = 8. Error bars display the SEM. *P < 0.05 vs. control.

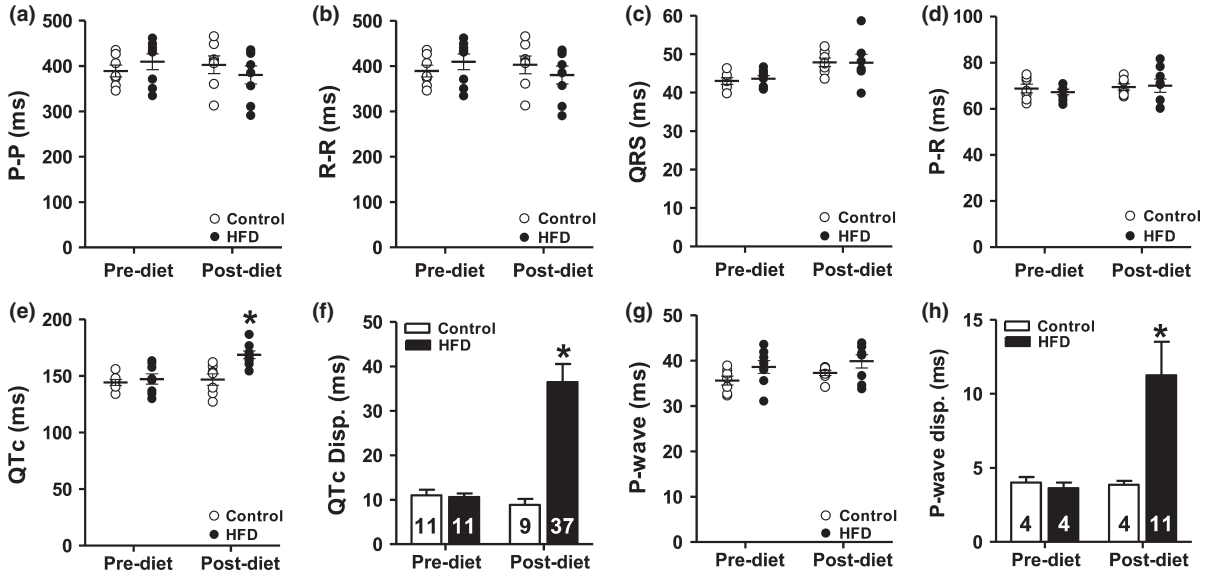

Figure 3 Modifications in the ECG produced by the HFD. P-P interval. (a) P-P interval, (b) R-R interval, (c) QRS duration, (d) P-R interval, (e) QTc, (f) QTc dispersion, (g) P-wave duration and (h) P-wave dispersion in control (n = 7) and HFD (n = 8) groups. Error bars display the SEM. *P < 0.05 vs. control.

and its dispersion were increased in the HFD group compared with controls (146 ± 13 vs. 169 ± 10 and 9 ± 4 vs. 37 ± 11 ms, respectively, P < 0.05, Fig. 3e, f). Similarly, P-wave dispersion was slightly increased in the HFD group (4 ± 1 vs. 11 ± 6 ms post diet, P < 0.05, Fig. 3 h), but no differences in P-wave duration were found.

HRV analyses were performed for the non-edited data that included only real sinus intervals to obtain reference values for the HRV parameters. Representative traces of the ECG recordings are shown in Fig. 4a. In the time domain analysis of the short-term R-R interval data, we found no differences in any parameter studied (RR SD, RMS SD, pNN50) when comparisons were made between groups after starting the diet. In contrast, these parameters increased significantly (P < 0.01) in the HFD group by the end of the study (Fig. 4c). A similar trend was observed in the rest of parameters in the geometrical analysis (HRVI and TIRR), and the standard descriptors (SD1, SD2) of the Poincaré Plot (Fig. 4b,c), which increased in the HFD group after the 18 weeks of high-fat feeding (P < 0.01 vs. control).

Echocardiographic characteristics

Table 2 summarizes all relevant echocardiographic parameters studied. Systolic function was preserved in HFD rabbits as evidenced by no apparent change in both fractional shortening (33 ± 3 vs. 34 ± 5%) and ejection fraction (58 ± 7 vs. 59 ± 6%). In agreement with this, there was no significant change in heart rate (154 ± 13 vs. 145 ± 13 bpm), stroke volume (1308 ± 282 vs. 1411 ± 207 μL) and cardiac output (946 ± 485 vs. 798 ± 192 mL min^{-1}). However, HFD rabbit hearts developed a significant increase in LV mass when comparisons were made with their pre-diet values (3679 ± 488 vs. 5550 ± 1372 mg, P < 0.001). Also of note, there was a strong trend towards an increase in LV mass when comparisons were made between control and HFD group at the end of the study (4573 ± 953 vs. 5550 ± 1372 mg, P = 0.067), and LV mass indexed to height (LV mass per $height^{2.7}$), which has been used as an indicator of LV hypertrophy (Mukerji *et al.* 2012b), was significantly increased in the HFD group (42.5 ± 5.74 vs. 54.2 ± 13.4, P < 0.05). We also observed significant increase in interventricular (IV) septum thickness in diastole (2.5 ± 0.3 vs. 3.0 ± 0.5 mm, P < 0.05) and LV posterior wall thickness in diastole (2.1 ± 0.3 vs. 3.0 ± 0.9 mm, P < 0.05) in HFD hearts compared with controls, respectively. LA size significantly increased in HFD hearts after diet, compared with the pre-diet values (9.1 ± 1.1 vs. 10.9 ± 0.8 mm, P < 0.01) and also showed a trend for an increase when compared with controls at the end of the study (10.9 ± 0.8 vs. 9.2 ± 1.2 mm, P = 0.091). Interestingly, while mitral A wave velocity decreased with time at the end of the study in control hearts (313 ± 50 vs. 204 ± 90 mm mg^{-1} s^{-1}, P < 0.01), it was maintained in the HFD group throughout the study (251 ± 62 vs. 252 ± 127 mm s^{-1}). Of note, there was no significant change in other measurements of diastolic function such as IVRT (50 ± 13 vs.

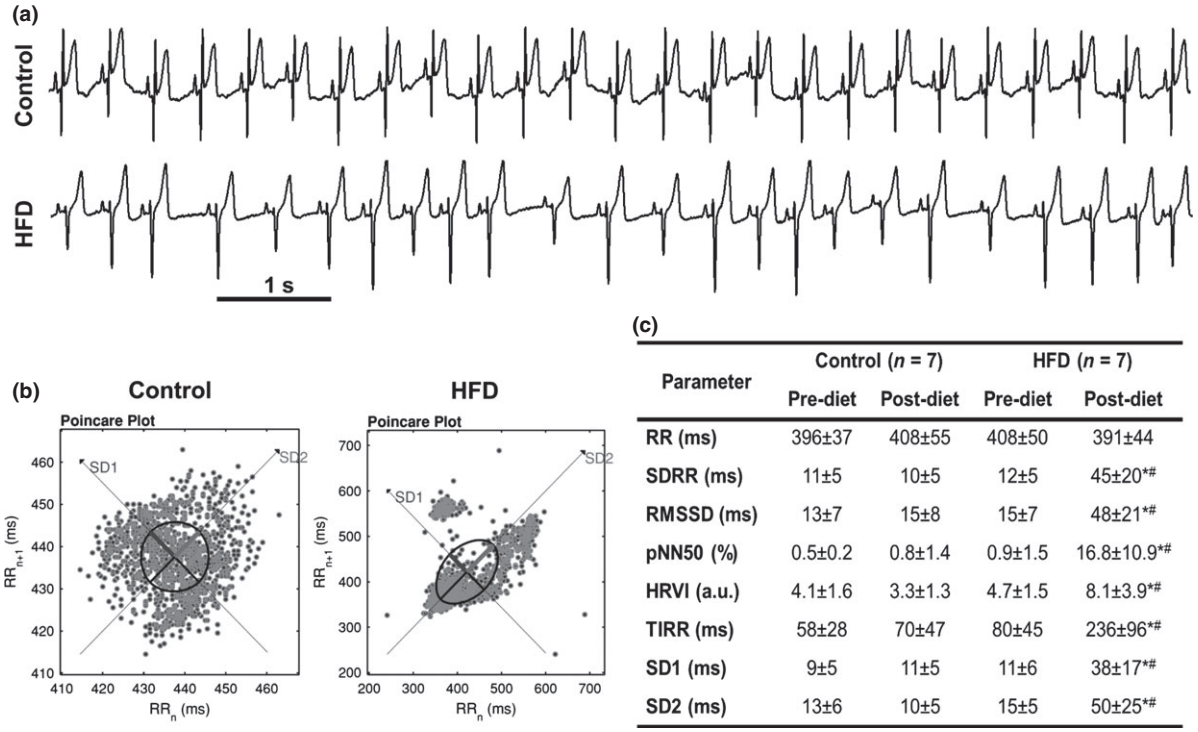

(c)

Parameter	Control (n = 7)		HFD (n = 7)	
	Pre-diet	Post-diet	Pre-diet	Post-diet
RR (ms)	396±37	408±55	408±50	391±44
SDRR (ms)	11±5	10±5	12±5	45±20*#
RMSSD (ms)	13±7	15±8	15±7	48±21*#
pNN50 (%)	0.5±0.2	0.8±1.4	0.9±1.5	16.8±10.9*#
HRVI (a.u.)	4.1±1.6	3.3±1.3	4.7±1.5	8.1±3.9*#
TIRR (ms)	58±28	70±47	80±45	236±96*#
SD1 (ms)	9±5	11±5	11±6	38±17*#
SD2 (ms)	13±6	10±5	15±5	50±25*#

Figure 4 Short-term HRV analysis of the R-R interval series. (a) Representative traces of 10 s ECG signals in control and HFD groups after 18 weeks of high-fat feeding. (b) Beat-to-beat graphical representation (Poincaré plot) in control and HFD at the end of the study. (c) Parameters of HRV analysis. Data are expressed as mean ± SD. *$P < 0.01$ vs. control; #$P < 0.01$ vs. pre-diet.

44 ± 8 ms), mitral E wave velocity (451 ± 80 vs. 484 ± 59 ms), E/E' ratio (8.3 ± 4.7 vs. 10.2 ± 4.7) or E/A ratio (1.9 ± 0.5 vs. 2.3 ± 0.9).

Electrophysiological studies in isolated hearts

Optical mapping was used to record electrical activity in the ventricle of Langendorff-perfused hearts. When the heart was perfused with Tyrode under physiological extracellular K^+ concentration ($[K^+]_o$) = 4 mmol L^{-1}, the mean APD_{80} values were not different between the two experimental groups at all pacing frequencies explored (Fig. 5a): 137 ± 3 vs. 131 ± 5 ms at 250 ms CL, 131 ± 4 vs. 129 ± 3 ms at 225 ms CL, 126 ± 3 vs. 123 ± 3 ms at 200 ms CL, 119 ± 1 vs. 116 ± 3 ms at 175 ms CL and 109 ± 1 vs. 108 ± 3 ms at 150 ms CL, in control (n = 6) and HFD (n = 7) groups, respectively. Similarly, no differences were seen in CV at any of the different pacing frequencies studied between control and HFD groups: 0.68 ± 0.08 vs. 0.65 ± 0.09 m s^{-1} at 250 ms CL, 0.69 ± 0.08 vs. 0.65 ± 0.09 m s^{-1} at 225 ms CL, 0.69 ± 0.07 vs. 0.65 ± 0.09 m s^{-1} at 200 ms CL, 0.67 ± 0.07 vs. 0.64 ± 0.08 m s^{-1} at 175 ms CL and 0.67 ± 0.07 vs. 0.63 ± 0.08 m s^{-1} at 150 ms CL (Fig. 5d).

The hearts were subsequently studied under conditions of hyperkalaemia ($[K^+]_o$ = 12 mmol L^{-1}). The expected shortening in the APD_{80}, and a reduction in CV in hyperkalaemia compared with normokalaemia was observed in both groups. Under these conditions, we obtained a small but significant decrease in APD_{80} in the HFD group with increasing pacing CL (Fig. 5b): 119 ± 4 vs. 118 ± 3 ms at 250 ms CL, 117 ± 4 vs. 112 ± 3 ms at 225 ms CL (P = 0.11), 113 ± 3 vs. 107 ± 2 ms at 200 ms CL ($P < 0.05$) and 108 ± 1 vs. 102 ± 2 ms at 175 ms CL ($P < 0.05$), in control (n = 6) and HFD (n = 5) groups, respectively. In contrast, no differences were observed in CV at any of the different pacing frequencies studied: 0.44 ± 0.09 vs. 0.46 ± 0.09 m s^{-1} at 250 ms CL, 0.41 ± 0.09 vs. 0.43 ± 0.09 m s^{-1} at 225 ms CL, 0.39 ± 0.08 vs. 0.41 ± 0.09 m s^{-1} at 200 ms CL and 0.35 ± 0.09 vs. 0.37 ± 0.09 m s^{-1} at 175 ms CL (Fig. 5e) in control vs. HFD groups, respectively. Interestingly, at increased extracellular K^+ concentrations (12 mmol L^{-1}), arrhythmic episodes were observed after pacing in four of eight hearts in the HFD group, vs. in zero of seven hearts in the control group.

The heart was then challenged with 100 nmol L^{-1} isoproterenol (in normokalaemia). Under these condi-

Table 2 Echocardiographic data before (pre) and after 18 weeks of high-fat diet (post) feeding

	Control		HFD	
	Pre	Post	Pre	Post
Haemodynamics				
Heart rate (bpm)	157 ± 29	145 ± 13	148 ± 22	154 ± 13
Stroke volume (μL)	1512 ± 406	1411 ± 207	1632 ± 438	1308 ± 282
Cardiac output (mL min^{-1})	766 ± 612	798 ± 192	1115 ± 890	946 ± 485
Systolic function				
LV ejection fraction (%)	56 ± 9	59 ± 6	54 ± 4	59 ± 7
LV volume diastole (μL)	1507 ± 599	1432 ± 149	1130 ± 159	1091 ± 456
LV volume systole (μL)	564 ± 154	593 ± 125	517 ± 105	503 ± 130
LV fractional shortening (%)	32 ± 6	34 ± 5	30 ± 3	33 ± 3
LV int. diameter diastole (mm)	14.3 ± 9	15.4 ± 0.8	13.7 ± 0.9	14.1 ± 1.2*
LV int. diameter systole (mm)	9.8 ± 1.4	10.2 ± 1.0	9.6 ± 0.9	9.4 ± 1.1
Diastolic function				
Mitral valve E vel. (mm s^{-1})	484 ± 83	482 ± 75	451 ± 80	484 ± 59
Mitral valve A vel. (mm s^{-1})	313 ± 50	204 ± 90†	251 ± 62	252 ± 127
E' septal annulus vel. (mm s^{-1})	57 ± 13	65 ± 14	65 ± 25	54 ± 18
Mitral valve E/A	1.6 ± 0.5	2.6 ± 0.7†	1.9 ± 0.5	2.3 ± 0.9
Mitral valve E/E'septal annulus	9.5 ± 4.1	8.3 ± 4.7	8.4 ± 1.8	10.2 ± 4.7
Isovolumic relax. time (ms)	52 ± 27	50 ± 13	49 ± 11	44 ± 8
Isovolumic cont. time (ms)	57 ± 19	54 ± 30	51 ± 15	46 ± 24
Morphological parameters				
IVS diastole (mm)	2.3 ± 0.3	2.5 ± 0.3	2.3 ± 0.3	3.0 ± 0.5‡*
IVS systole (mm)	3.5 ± 0.5	3.7 ± 0.5	3.4 ± 0.3	4.2 ± 0.8‡
LV posterior wall diastole (mm)	2.2 ± 0.3	2.1 ± 0.3	2.2 ± 0.3	3.0 ± 0.9‡*
LV posterior wall systole (mm)	564 ± 154	593 ± 125	517 ± 105	503 ± 130
LV mass (mg)	3840 ± 400	4573 ± 953	3679 ± 488	5550 ± 1372‡§
LV mass per $height^{2.7}$ (g per $m^{2.7}$)	–	42.5 ± 5.74	–	54.2 ± 13.4*
LA size (mm)	9.2 ± 1.2	10.1 ± 0.6	9.1 ± 1.1	10.9 ± 0.8‡¶
LA size increase (%)	–	10 ± 11	–	21 ± 23
LA volume (μL)	440 ± 201	510 ± 135	504 ± 124	606 ± 134

LV, left ventricle; IVS, interventricular septum; LA, left atria. Data are presented as mean ± SD.
*$P < 0.05$.
†$P < 0.05$ control pre-diet vs. post-diet.
‡$P < 0.05$ HFD pre-diet vs. post-diet.
§$P = 0.06$.
¶$P = 0.09$ control vs. HFD post diet.

tions, we did not find any difference in APD_{80} (Fig. 5c) and CV (Fig. 5f) between control and HFD group. In this set of experiments, APD_{80} values were 90 ± 7 vs. 92 ± 2 ms at 150 ms CL, 82 ± 7 vs. 83 ± 3 ms at 125 ms CL and 71 ± 5 vs. 71 ± 2 ms at 100 ms CL, in control ($n = 6$) and HFD hearts ($n = 5$), respectively. The values of CV were 0.71 ± 0.09 m s^{-1} at 150 ms CL, 0.68 ± 0.09 m s^{-1} at 125 ms CL and 0.68 ± 0.08 m s^{-1} at 100 ms CL in the control group, and 0.70 ± 0.09 m s^{-1}, 0.68 ± 0.08 m s^{-1} and 0.67 ± 0.07 m s^{-1} at 150, 125 and 100 ms CL, respectively, in the HFD group.

Ventricular fibrillation (VF) was induced in the presence of isoproterenol, by pacing at increasing frequencies until sustained arrhythmia was obtained, and optical movies were recorded for 6 min to obtain information about the characteristics of the VF dynamics (for a detailed description of the parameters, see Supplemental methods). We first quantified the dominant frequency (DF) of excitation over the surface of the heart. In the control group, DF was 16.48 ± 1.63 Hz ($n = 5$) 30 s after VF initiation, and decreased to 15.31 ± 0.96 after 6 min. The same trend was observed in the HFD group ($n = 8$), where DF reached values of 16.89 ± 0.98 Hz just after the initiation of the arrhythmia (30 s) and decreased to 15.94 ± 0.95 Hz in the last time point studied (360 s). There were no significant differences in DF values between the two groups (Fig. 6a). We then studied the regularity index (RI), a parameter that

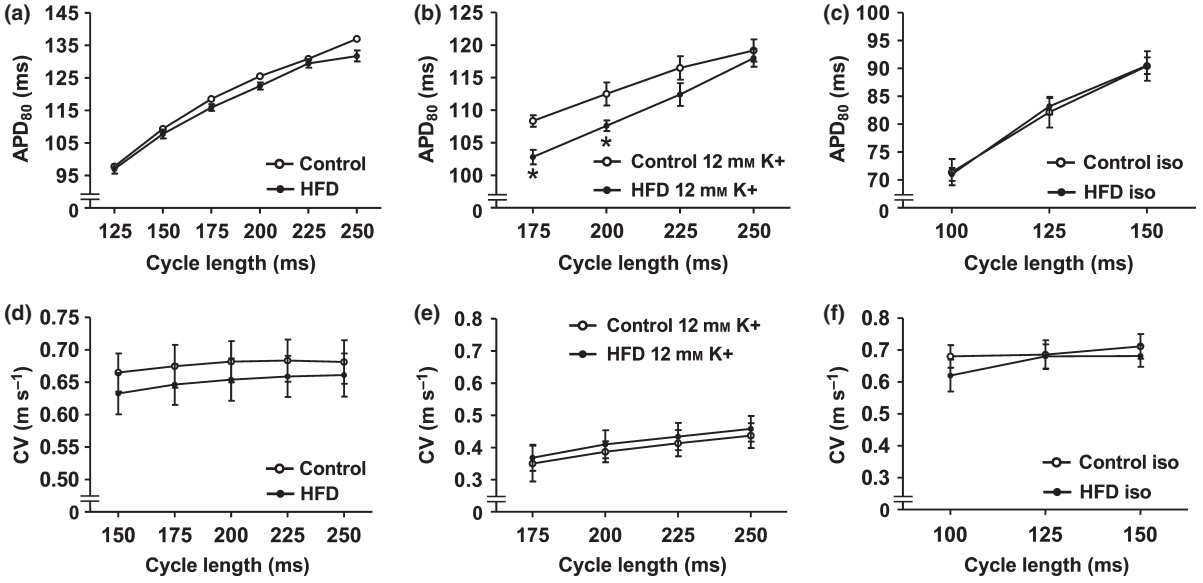

Figure 5 Optical mapping of the isolated heart. (a) Action potential duration at 80% of repolarization (APD80) in the ventricle of hearts perfused with normal Tyrode's solution, (b) during hyperkalaemia and (c) during isoproterenol perfusion. In panels d-e, we can observe the values of conduction velocity during normal Tyrode (d), hyperkalaemia (e) and isoproterenol perfusion (f). Norrmal Tyrode: control (n = 7), HFD (n = 8); hyperkalaemia: control (n = 6), HFD (n = 5), isoproterenol: control (n = 7), HFD (n = 5). Error bars display the SEM. *$P < 0.05$.

describes how the different frequencies of VF are distributed around the DF (Kalifa *et al.* 2006) and found no differences between control and HFD hearts (Fig. 6c) RI in controls was 0.174 ± 0.06 and 0.178 ± 0.05, whereas in HFD hearts, the RI values were 0.182 ± 0.10 and 0.178 ± 0.054, 30 s after VF triggering and after 360 s of the arrhythmia, respectively. Finally, we constructed phase movies to identify the phase singularities and quantify the singularity point density (SPD) at the sites of wave break (Pandit *et al.* 2010). Control and HFD hearts showed a similar degree of VF organization and the SPD was 7.64 ± 1.95 sp mm^{-2} vs. 8.88 ± 3.03 sp mm^{-2} at 30 s, and 10.82 ± 3.56 sp mm^{-2} vs. 8.92 ± 2.73 sp mm^{-2} at 360 s, in control and HFD groups, respectively (Fig. 6b).

Discussion

The main findings from our study are as follows: (i) a sustained diet-induced weight gain in HFD rabbits during 18 weeks induces a type-2 diabetic phenotype, which is associated with an increased LV mass and hypertrophy, and a trend towards diastolic dysfunction in some parameters, but no changes in systolic function. (ii) ECG recordings obtained *in vivo* reveal a prolonged QTc interval, and enhanced dispersion of QTc in HFD rabbits compared with controls. The P-wave dispersion was also slightly increased. Other ECG parameters remain unchanged. (iii) Optical imaging studies reveal no changes in either the APD or CV in normal extracellular K^+, or in the response to isoproterenol, including the dynamics of VF, between control and HFD rabbits. However, HFD rabbits show a small reduction in APD and an increased incidence of ventricular arrhythmias during hyperkalaemia, compared with controls.

Previous studies have mainly utilized rodent models of diet-induced obesity to study the effect on the electrophysiological remodelling in the heart. In the obese Zucker rat model, APD prolongation was reported and was mainly attributed to abnormal inactivation of the L-type Ca^{2+} current, I_{CaL} (Lin *et al.* 2012). In contrast, another study in which rats were fed with high calorie diet for 14 weeks, did not find any changes in either I_{CaL}, or any other K^+ currents or exchangers in isolated left ventricular myocytes (Ricci *et al.* 2006). In a recent study of diet-induced obesity in mice, QT prolongation was observed and attributed to a reduced expression of Kv1.5 channels in the ventricle (Huang *et al.* 2013). However, in higher animal models like rabbit and canine, as well as in man, Kv1.5 does not play any role in ventricular repolarization and is found only in the atrial tissue (Nerbonne & Kass 2005). In a model of metabolic syndrome obtained via sustained high fructose/sucrose diet in guinea pig hearts, no APD prolongation (measured via monophasic action potential recordings) was found compared with control hearts despite weight gain (Caillier *et al.* 2012), which is similar to our observations in isolated rabbit

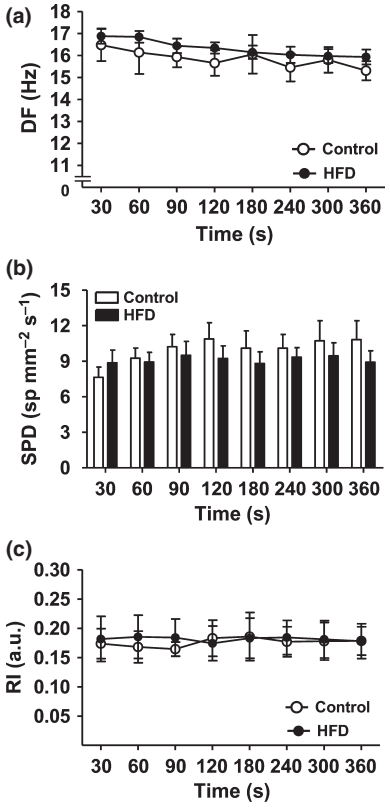

Figure 6 Characteristics of the isoproterenol-induced ventricular fibrillation (VF). (a), comparison of the dominant frequency (DF) of VF, (b) singularity points density (SPD) and (c) the regularity index (RI) of VF. Control $n = 5$, HFD $n = 8$. Sustained VF could not be induced in 2 control hearts. Error bars display the SEM.

heart studies. However, no *in vivo* ECG studies were conducted in these guinea pigs.

In lieu of the varied reports in the literature, we sought to develop and study a clinically relevant model of obese rabbits (Carroll *et al.* 1996), where the ventricular electrophysiology is similar to humans (Nerbonne & Kass 2005). In our model, we observed a 25% increase in body weight and BMI, compared with approx. 45% increase in body weight reported by Carroll *et al.* (1996) in their studies. The exact reason for this discrepancy is not clear, but could be related to the use of younger, male rabbits in our study compared with older, female rabbits in Carrol's study. Our changes in QTc with increased weight are line with clinical reports that suggest similar findings in obese patients (Girola *et al.* 2001, Mukerji *et al.* 2012a). These studies have also reported that QTc prolongation correlates with an increased LV mass (Mukerji *et al.* 2012b), which is also increased in our rabbit obese model. In addition, taken together, all significant echocardiographic changes observed in HFD hearts (increased LV mass, increased LVPWT, increased IVST) point to the development of concentric LV hypertrophy with a preserved EF and FS. However, while systolic function was preserved, the HFD hearts appeared to develop a trend towards a very mild diastolic dysfunction as there was a significant increase in LA size (which could suggest increased LV filling pressures), and a higher dependence on atrial contraction for diastolic filling (as evidenced by a maintenance in mitral A wave velocity in HFD hearts which normally decreased in controls throughout the experiment). Our findings correlate well with what others have observed with similar HFD rabbits (Carroll *et al.* 1997) and other or genetic obesity models in animal species (Abel *et al.* 2008, Murase *et al.* 2012). Of note, the changes in diastolic function we observed were mild as evidenced by no significant changes in other relevant measurements such as IVRT, mitral E wave velocity, E/A ratio or E/E' ratio. Given the short duration of the HFD, we could speculate this to be a time dependent effect and diastolic dysfunction would worsen as time with HFD feeding regime increases.

Regarding the HRV analysis of the ECG data, we found a marked increase in all the parameters (statistical and geometrical) in the time domain of the short-term R-R series (Fig. 4c), reflecting a higher variability in the HFD group after 18 weeks of high-fat feeding. All these measurements estimate high-frequency variations and thus are highly correlated with parasympathetic activity (Kawada *et al.* 2013). Indeed, it is well established that the high-frequency component of R-R interval variability primarily reflects the vagal modulation of the respiratory sinus arrhythmia (RSA) (Malik 1996). In Fig. 4a, we can observe arrhythmic episodes that were common in the HFD group. Of note, ECG recordings were performed under anaesthesia, and in those conditions, animals in the HFD group were more susceptible to the appearance of arrhythmic episodes, possibly reflecting an altered pattern of RSA by increased parasympathetic activity.

Nevertheless, our data indicate that there is little or no electrical remodelling at the isolated heart level, as shown by the analysis of the volume-conducted ECG (Supplemental Figure S1) and the APD/CV analysis from the optical mapping experiments. The rabbit obese model was studied in contrast to rodent models, because the delayed rectifier K^+ currents are present in rabbits, but absent in rodents. If the fast delayed rectifier K^+ current, I_{Kr}, was downregulated in obese rabbits, the APD would have been prolonged in the Langendorff experiments in normokalaemia, as I_{Kr} is the main repolarizing current in the rabbit ventricle. Further if the slow delayed rectifier current, I_{Ks}, was downregulated in obese rabbits, this would have displayed different APD in response to isoproterenol, as

I_{Ks} is mainly active during adrenergic stress. Thus, our results indicate that likely the densities of I_{Kr} and I_{Ks} are not altered in these obese rabbits. However, ionic/molecular studies are necessary to confirm this hypothesis. Further, this also suggests that either autonomic nervous system remodelling, circulating free fatty acids or increased ventricular load might contribute to the observed *in vivo* changes in QTc. Previous studies in obese rabbits showed a reduced plasma K^+ concentration (Carroll *et al.* 1996), which could further contribute to QTc prolongation. However, further experiments will be necessary to test this hypothesis. The increased P-wave dispersion seen in HFD rabbits has also been seen in obese patients (Seyfeli *et al.* 2006), and this may be associated with increased risk of atrial fibrillation (Kosar *et al.* 2008, King *et al.* 2013).

Our results also show no changes in the response of HFD hearts to isoproterenol or VF characteristics, compared to control hearts. This indicates that at this stage, the adrenergic electrophysiological response in the intact myocardium is not impaired. Interestingly, our data suggest that high-frequency pacing in the presence of hyperkalaemia shows a shortening of the APD, and more arrhythmia patterns in HFD rabbits, compared with controls. The exact underlying mechanisms are not clear and could be related to changes in the expression or function of the Na^+-K^+ pump, and the Na^+-Ca^{2+} exchanger, or other ion channels that may disrupt ion exchange and homoeostasis. Further studies are necessary at the ionic/molecular level to understand these differences.

Our optical imaging studies have been conducted in the presence of blebbistatin, to suppress heart contraction and motion artefact. We have also not conducted studies of intracellular Ca^{2+} transient properties, which may be altered, and explain the trend towards diastolic dysfunction in HFD rabbits (Lacombe *et al.* 2007, Miklós *et al.* 2012, Shi *et al.* 2013). The ECG measurements were performed in the presence of anaesthesia in both groups, but we cannot rule out completely the effects of the anaesthetics on the ECG. However, the QT intervals were corrected to compensate for changes on heart rate. Despite these limitations, our study presents the first detailed characterization of electrophysiological alterations occurring in obese rabbits, which may have important implications for cardiac pathophysiology, arrhythmias, and their treatment.

Conflict of interest

Sandeep V. Pandit is a recipient of a grant from Gilead Sciences. The rest of authors have no conflict of interests to declare.

This study was supported by the Generalitat Valenciana grant PROMETEO 2010/093 to MZ and by Gilead Inc. and University of Michigan Internal funds (courtesy Dr. David Pinsky/Dr. José Jalife) to SVP. The authors thank Kimber Converso-Baran, Jiang Jiang and Jesús Zarzoso for their excellent technical assistance. The authors gratefully acknowledge useful discussions with Dr. José Jalife, Dr. Sub Pennathur, and Dr. Bertram Pitt.

References

Abel, E.D., Litwin, S.E. & Sweeney, G. 2008. Cardiac remodeling in obesity. *Physiol Rev* **88**, 389–419.

Brines, L., Such-Miquel, L., Gallego, D., Trapero, I., Del Canto, I., Zarzoso, M., Soler, C., Pelechano, F., Cánoves, J., Alberola, A., Such, L. & Chorro, F.J. 2012. Modifications of mechanoelectric feedback induced by 2,3-butanedione monoxime and Blebbistatin in Langendorff-perfused rabbit hearts. *Acta Physiol (Oxf)* **206**, 29–41.

Caillier, B., Pilote, S., Patoine, D., Levac, X., Couture, C., Daleau, P., Simard, C. & Drolet, B. 2012. Metabolic syndrome potentiates the cardiac action potential-prolonging action of drugs: a possible 'anti-proarrhythmic' role for amlodipine. *Pharmacol Res* **65**, 320–327.

Carroll, J.F., Dwyer, T.M., Grady, A.W., Reinhart, G.A., Montani, J.P., Cockrell, K., Meydrech, E.F. & Mizelle, H.L. 1996. Hypertension, cardiac hypertrophy, and neurohumoral activity in a new animal model of obesity. *Am J Physiol* **271**, H373–H378.

Carroll, J.F., Braden, D.S., Cockrell, K. & Mizelle, H.L. 1997. Obese hypertensive rabbits develop concentric and eccentric hypertrophy and diastolic filling abnormalities. *Am J Hypertens* **10**, 230–233.

Fedorov, V.V., Lozinsky, I.T., Sosunov, E.A., Anyukhovsky, E.P., Rosen, M.R., Balke, C.W. & Efimov, I.R. 2007. Application of blebbistatin as an excitation-contraction uncoupler for electrophysiologic study of rat and rabbit hearts. *Heart Rhythm* **4**, 619–626.

Fraley, M.A., Birchem, J.A., Senkottaiyan, N. & Alpert, M.A. 2005. Obesity and the electrocardiogram. *Obes Rev* **6**, 275–281.

Girola, A., Enrini, R., Garbetta, F., Tufano, A. & Caviezel, F. 2001. QT dispersion in uncomplicated human obesity. *Obes Res* **9**, 71–77.

Herron, T.J., Devaney, E., Mundada, L., Arden, E., Day, S., Guerrero-Serna, G., Turner, I., Westfall, M. & Metzger, J.M. 2010. Ca2 + -independent positive molecular inotropy for failing rabbit and human cardiac muscle by alpha-myosin motor gene transfer. *FASEB J* **24**, 415–424.

Huang, H., Amin, V., Gurin, M., Wan, E., Thorp, E., Homma, S. & Morrow, J.P. 2013. Diet-induced obesity causes long QT and reduces transcription of voltage-gated potassium channels. *J Mol Cell Cardiol* **59**, 151–158.

Kalifa, J., Tanaka, K., Zaitsev, A.V., Warren, M., Vaidyanathan, R., Auerbach, D., Pandit, S., Vikstrom, K.L., Ploutz-Snyder, R., Talkachou, A., Atienza, F., Guiraudon, G., Jalife, J. & Berenfeld, O. 2006. Mechanisms of wave fractionation at boundaries of high-frequency excitation in the

posterior left atrium of the isolated sheep heart during atrial fibrillation. *Circulation* **113**, 626–633.

Kannel, W.B., Plehn, J.F. & Cupples, L.A. 1988. Cardiac failure and sudden death in the Framingham Study. *Am Heart J* **115**, 869–875.

Kawada, T., Li, M., Shimizu, S., Kamiya, A., Uemura, K., Turner, M.J., Mizuno, M. & Sugimachi, M. 2013. High-frequency dominant depression of peripheral vagal control of heart rate in rats with chronic heart failure. *Acta Physiol (Oxf)* **207**, 494–502.

Killeen, M.J., Thomas, G., Sabir, I.N., Grace, A.A. & Huang, C.L. 2008. Mouse models of human arrhythmia syndromes. *Acta Physiol (Oxf)* **192**, 455–469.

King, J.H., Zhang, Y., Lei, M., Grace, A.A., Huang, C.L. & Fraser, J.A. 2013. Atrial arrhythmia, triggering events and conduction abnormalities in isolated murine RyR2-P2328S hearts. *Acta Physiol (Oxf)* **207**, 308–323.

Koike, T., Liang, J., Wang, X., Ichikawa, T., Shiomi, M., Liu, G., Sun, H., Kitajima, S., Morimoto, M., Watanabe, T., Yamada, N. & Fan, J. 2004. Overexpression of lipoprotein lipase in transgenic Watanabe heritable hyperlipidemic rabbits improves hyperlipidemia and obesity. *J Biol Chem* **279**, 7521–7529.

Kosar, F., Aksoy, Y., Ari, F., Keskin, L. & Sahin, I. 2008. P-wave duration and dispersion in obese subjects. *Ann Noninvasive Electrocardiol* **13**, 3–7.

Lacombe, V.A., Viatchenko-Karpinski, S., Terentyev, D., Sridhar, A., Emani, S., Bonagura, J.D., Feldman, D.S., Györke, S. & Carnes, C.A. 2007. Mechanisms of impaired calcium handling underlying subclinical diastolic dysfunction in diabetes. *Am J Physiol Regul Integr Comp Physiol* **293**, R1787–R1797.

Lakhani, M. & Fein, S. 2011. Effects of obesity and subsequent weight reduction on left ventricular function. *Cardiol Rev* **19**, 1–4.

Lavie, C.J., Milani, R.V. & Ventura, H.O. 2009. Obesity and cardiovascular disease: risk factor, paradox, and impact of weight loss. *J Am Coll Cardiol* **53**, 1925–1932.

Lengyel, C., Iost, N., Virág, L., Varró, A., Lathrop, D.A. & Papp, J.G. 2001. Pharmacological block of the slow component of the outward delayed rectifier current (I (Ks)) fails to lengthen rabbit ventricular muscle QT(c) and action potential duration. *Br J Pharmacol* **132**, 101–110.

Lengyel, C., Virág, L., Kovács, P.P., Kristóf, A., Pacher, P., Kocsis, E., Koltay, Z.M., Nánási, P.P., Tóth, M., Kecskeméti, V., Papp, J.G., Varró, A. & Jost, N. 2008. Role of slow delayed rectifier K + -current in QT prolongation in the alloxan-induced diabetic rabbit heart. *Acta Physiol (Oxf)* **192**, 359–368.

Lin, Y.C., Huang, J., Kan, H., Castranova, V., Frisbee, J.C. & Yu, H.G. 2012. Defective calcium inactivation causes long QT in obese insulin-resistant rat. *Am J Physiol Heart Circ Physiol* **302**, H1013–H1022.

Liu, E., Kitajima, S., Higaki, Y., Morimoto, M., Sun, H., Watanabe, T., Yamada, N. & Fan, J. 2005. High lipoprotein lipase activity increases insulin sensitivity in transgenic rabbits. *Metabolism* **54**, 132–138.

Malik, M. 1996. Heart rate variability: standards of measurement, physiological interpretation and clinical use. Task Force of the European Society of Cardiology and the North American Society of Pacing and Electrophysiology. *Circulation* **93**, 1043–1065.

Messerli, F.H., Nunez, B.D., Ventura, H.O. & Snyder, D.W. 1987. Overweight and sudden death. Increased ventricular ectopy in cardiopathy of obesity. *Arch Intern Med* **147**, 1725–1728.

Miklós, Z., Kemecsei, P., Bíró, T., Marincsák, R., Tóth, B.I., Op den Buijs, J., Benis, É., Drozgyik, A. & Ivanics, T. 2012. Early cardiac dysfunction is rescued by upregulation of SERCA2a pump activity in a rat model of metabolic syndrome. *Acta Physiol (Oxf)* **205**, 381–393.

Mukerji, R., Petruc, M., Fresen, J.L., Terry, B.E., Govindarajan, G. & Alpert, M.A. 2012a. Effect of weight loss after bariatric surgery on left ventricular mass and ventricular repolarization in normotensive morbidly obese patients. *Am J Cardiol* **110**, 415–419.

Mukerji, R., Terry, B.E., Fresen, J.L., Petruc, M., Govindarajan, G. & Alpert, M.A. 2012b. Relation of left ventricular mass to QTc in normotensive severely obese patients. *Obesity* **20**, 1950–1954.

Murase, T., Hattori, T., Ohtake, M., Abe, M., Amakusa, Y., Takatsu, M., Murohara, T. & Nagata, K. 2012. Cardiac remodeling and diastolic dysfunction in DahlS.Z-Lepr(fa)/Lepr(fa) rats: a new animal model of metabolic syndrome. *Hypertens Res* **35**, 186–193.

Nduhirabandi, F., du Toit, E.F. & Lochner, A. 2012. Melatonin and the metabolic syndrome: a tool for effective therapy in obesity-associated abnormalities? *Acta Physiol (Oxf)* **205**, 209–223.

Nerbonne, J.M. & Kass, R.S. 2005. Molecular physiology of cardiac repolarization. *Physiol Rev* **85**, 1205–1253.

Niskanen, J.P., Tarvainen, M.P., Ranta-aho, P.O. & Karjalainen, P.A. 2004. Software for advanced HRV analysis. *Comput Methods Programs Biomed* **76**, 73–81.

Noujaim, S.F., Stuckey, J.A., Ponce-Balbuena, D., Ferrer-Villada, T., López-Izquierdo, A., Pandit, S., Calvo, C.J., Grzeda, K.R., Berenfeld, O., Chapula, J.A. & Jalife, J. 2010. Specific residues of the cytoplasmic domains of cardiac inward rectifier potassium channels are effective antifibrillatory targets. *FASEB J* **24**, 4302–4312.

Pandit, S.V., Warren, M., Mironov, S., Tolkacheva, E.G., Kalifa, J., Berenfeld, O. & Jalife, J. 2010. Mechanisms underlying the antifibrillatory action of hyperkalemia in Guinea pig hearts. *Biophys J* **98**, 2091–2101.

Pandit, S.V., Kaur, K., Zlochiver, S., Noujaim, S.F., Furspan, P., Mironov, S., Shibayama, J., Anumonwo, J. & Jalife, J. 2011a. Left-to-right ventricular differences in I(KATP) underlie epicardial repolarization gradient during global ischemia. *Heart Rhythm* **8**, 1732–1739.

Pandit, S.V., Zlochiver, S., Filgueiras-Rama, D., Mironov, S., Yamazaki, M., Ennis, S.R., Noujaim, S.F., Workman, A.J., Berenfeld, O., Kalifa, J. & Jalife, J. 2011b. Targeting atrioventricular differences in ion channel properties for terminating acute atrial fibrillation in pigs. *Cardiovasc Res* **89**, 843–851.

Persson, P.B. & Henriksson, J. 2011. Good publishing practice in physiology. *Acta Physiol (Oxf)* **203**, 403–407.

Persson, A.B. & Persson, P.B. 2012. Cardiac electrophysiology: what is behind our two-billion heart beats? *Acta Physiol (Oxf)* **206**, 90–93.

Ricci, E., Smallwood, S., Chouabe, C., Mertani, H.C., Raccurt, M., Morel, G. & Bonvallet, R. 2006. Electrophysiological characterization of left ventricular myocytes from obese Sprague-Dawley rat. *Obesity* **14**, 778–786.

Seyfeli, E., Duru, M., Kuvandik, G., Kaya, H. & Yalcin, F. 2006. Effect of obesity on P-wave dispersion and QT dispersion in women. *Int J Obes (Lond)* **30**, 957–961.

Shi, C., Wang, X., Dong, F., Wang, Y., Hui, J., Lin, Z., Yang, J. & Xu, Y. 2013. Temporal alterations and cellular mechanisms of transmural repolarization during progression of mouse cardiac hypertrophy and failure. *Acta Physiol (Oxf)* **208**, 95–110.

Such, L., Alberola, A.M., Such-Miquel, L., López, L., Trapero, I., Pelechano, F., Gómez-Cabrera, M.C., Tormos, A., Millet, J. & Chorro, F.J. 2008. Effects of chronic exercise on myocardial refractoriness: a study on isolated rabbit heart. *Acta Physiol (Oxf)* **193**, 331–339.

Torres-Jacome, J., Gallego, M., Rodríguez-Robledo, J.M., Sanchez-Chapula, J.A. & Casis, O. 2013. Improvement of the metabolic status recovers cardiac potassium channel synthesis in experimental diabetes. *Acta Physiol (Oxf)* **207**, 447–459.

Van Gaal, L.F., Mertens, I.L. & De Block, C.E. 2006. Mechanisms linking obesity with cardiovascular disease. *Nature* **444**, 875–880.

Zarzoso, M., Such-Miquel, L., Parra, G., Brines-Ferrando, L., Such, L., Chorro, F.J., Guerrero, J., Guill, A., O'Connor, J.E. & Alberola, A. 2012. The training-induced changes on automatism, conduction and myocardial refractoriness are not mediated by parasympathetic postganglionic neurons activity. *Eur J Appl Physiol* **112**, 2185–2193.

Zarzoso, M., Rysevaite, K., Milstein, M.L., Calvo, C.J., Kean, A.C., Atienza, F., Pauza, D.H., Jalife, J. & Noujaim, S.F. 2013. Nerves projecting from the intrinsic cardiac ganglia of the pulmonary veins modulate sinoatrial node pacemaker function. *Cardiovasc Res* **99**, 566–575.

Zhang, X.J., Chinkes, D.L., Aarsland, A., Herndon, D.N. & Wolfe, R.R. 2008. Lipid metabolism in diet-induced obese rabbits is similar to that of obese humans. *J Nutr* **138**, 515–518.

Supporting Information

Additional Supporting Information may be found in the online version of this article:

Figure S1. Volume-conducted ECG parameters in optical mapping experiments.

Figure S2. Optical mapping data analysis and interpretation.

Figure S3. Dominant frequency (DF) analysis of the isoproterenol-induced ventricular fibrillation (VF).

Figure S4. Analysis of the spectral characteristics of the arrhythmia: regularity index and phase maps.

Table S1. Composition and calories provided by the standard and high-fat chows.

Table S2. Description of the echocardiographic measurements.

Table S3. Description of the short-term HRV measurements.

